Collisions of NO(X 2Π) with a Ag(111) surface: New quantum scattering studies based on a semiempirical potential energy surface

Millard H. Alexander

Citation: The Journal of Chemical Physics **94**, 8468 (1991); doi: 10.1063/1.460080
View online: http://dx.doi.org/10.1063/1.460080
View Table of Contents: http://scitation.aip.org/content/aip/journal/jcp/94/12?ver=pdfcov
Published by the AIP Publishing

Collisions of NO($X\,^2\Pi$) with a Ag(111) surface: New quantum scattering studies based on a semiempirical potential energy surface

Millard H. Alexander
Department of Chemistry, University of Maryland, College Park, Maryland 20742

(Received 15 November 1990; accepted 19 February 1991)

We report the results of fully quantum close-coupled studies of collisions of NO($X\,^2\Pi$) with a Ag(111) surface. The recent corrected effective medium potential energy surfaces (PES) of DePristo and Alexander [J. Chem. Phys. **94**, 8454 (1991)] were used. The final state rotational distributions show evidence of at least four rotational rainbows, corresponding to scattering on (and interference between) the two PES which arise when the degeneracy of the NO molecule is lifted upon approach to the surface. A strong tendency is seen to populate the lower spin–orbit manifold at low to moderate final J, which disappears as J rises beyond 30.5 and the final states are better described in Hund's case (b). Simultaneously, there exists a propensity to populate those Λ-doublet levels in which the electronic–rotational wave function is antisymmetric ($\Pi_{A''}$) with respect to reflection of the electronic coordinates in the plane of rotation of the scattered NO molecule. This feature is opposite to what has been seen experimentally. An approximate averaging over the lateral position of the NO molecule above the surface showed that although the rainbow oscillations are strongly sensitive to surface corrugation, the fine-structure propensities are not. This suggests that these latter are reflective of some fundamental characteristic of the NO–Ag interaction which is independent of the position of the NO molecule above the Ag(111) unit cell.

I. INTRODUCTION

There has been much recent theoretical interest in collisions of the NO molecule with the close-packed (111) face of a silver surface.[1-19] Because of the nonzero electronic orbital angular momentum of the ground $X\,^2\Pi$ electronic state of NO,[20] collisions of this molecule with a surface sample *two* potential energy surfaces (PES).[7,8] The interplay between these two PES, and the concomitant possibility of quantum interference effects, are manifested in the nonstatistical populations of the Λ-doublet and fine-structure levels of NO following both scattering[21-23] and desorption.[24,25] Interactions involving NO are qualitatively different from those involving a closed shell molecule such as CO or N_2, where only one PES is needed to describe the interaction of the molecule with a surface.

Despite the integral role played by the two PES in the scattering of NO, in most prior theoretical work the dynamics has been described in terms of only one PES.[1-6,9,10,14,15,19] An additional deficiency in all prior theoretical studies of the scattering dynamics is the reliance on model PES constructed intuitively, with parameters determined phenomenologically.

We have recently determined a new, semiempirical description of the interaction of NO with a Ag(111) surface.[26] The calculations described were based on the corrected effective medium (CEM) method of DePristo and coworkers.[27-31] Interaction energies between NO and the Ag(111) crystal were determined as a function of the orientation of both the nuclei and unpaired electron of this molecule, the distance of the center-of-mass of the molecule above the surface, and the location of the center-of-mass above the Ag(111) unit cell. The resulting ~ 600 calculated points were then fitted to a simple, yet accurate functional form.

In this paper we shall report fully quantum close coupled calculations for the scattering of NO by a Ag(111) surface, as described by the new PES of DePristo and Alexander (DA).[26] The present calculations are intended to show the importance of interference effects arising from the two PES and can additionally serve as benchmarks for the calibration of the accuracy of more approximate treatments of the dynamics. Toward this goal, we shall not arbitrarily adjust the PES to obtain a "best" fit of existing experimental data on the scattering of NO by silver surfaces.

The organization of this article is as follows: In Sec. II we reiterate the essential features of the discussion of the interaction potential given by DA. In Sec. III we review the scattering formalism and describe the scattering calculations. The results are contained in Secs. IV–VI, which present, respectively, the transition probabilities summed over fine-structure levels, the transition probabilities summed over just Λ-doublet levels, and the transition probabilities summed over just the two spin–orbit manifolds. These calculations were carried out for a flat surface, using *the surface* average interaction potential. In Sec. VII we investigate the site dependence of the final state distributions of the scattered molecules. A comparison with previous work is contained in Sec. VIII. A brief discussion follows.

II. DESCRIPTION OF POTENTIAL SURFACES

The formal therapy of the scattering of a molecule in a $^2\Pi$ electronic state by a flat surface was developed by Alexander[7] and Corey and Liu.[8] These initial papers were then

 0021-9606/91/128468-11$03.00

followed by several applications and extensions.[11-13,16-18,23] We refer the reader to these articles for a full development of the theory, restricting ourselves here to those details pertinent to the present discussion.

In a single reference description the electronic wave function of the NO molecule can be written as

$$|+\rangle = 1\sigma^2 2\sigma^2 3\sigma^2 4\sigma^2 5\sigma^2 1\pi^4 2\pi_y \tag{1a}$$

or

$$|-\rangle = 1\sigma^2 2\sigma^2 3\sigma^2 4\sigma^2 5\sigma^2 1\pi^4 2\pi_x. \tag{1b}$$

We choose the molecular frame coordinate system so that when the molecular axis lies in the plane of the surface, the π_y orbitals are oriented in the plane of the surface, while the π_x orbitals are oriented along the surface normal. When the molecule is rotated out of the plane of the surface through an angle γ, the π_y orbital will continue to remain parallel to the plane of the surface, while the π_x orbital will be oriented at an angle of γ with respect to the surface normal. The + and − designations indicate that when the molecular axis is parallel to the surface, the $|+\rangle$ wave function is *symmetric*, and the $|-\rangle$ wave function *antisymmetric*, with respect to reflection of the electronic coordinates in a plane parallel to the surface.

The interaction energy between the Ag surface and an NO molecule in states $|+\rangle$ and $|-\rangle$ will, in general, be the same only when the molecule is oriented perpendicular to the surface. For this reason two potential energy surfaces (PES) are required for a complete description of the interaction. This is a consequence of the directional properties of the singly filled 2π antibonding orbital of the NO molecule and will not arise for a molecule in a $^1\Sigma$ electronic state (as, for example, N_2 or CO). We shall denote by $V_+(X,Y,Z,\theta,\phi)$ and $V_-(X,Y,Z,\theta,\phi)$ the interaction potentials in the case where the singly filled π orbital lies, respectively, parallel and perpendicular to the surface, in orientations where the molecular axis lies parallel to the plane of the surface ($\theta = \pi/2$). Here, X, Y, Z designate the location of the center of mass of the NO molecule with respect to the surface, with the XY plane defining the plane of the surface. The polar angles θ, ϕ define the orientation of the NO molecular axis with respect to the surface normal.

As discussed earlier,[26] the dependence on the azimuthal angle ϕ of both the V_+ and V_- NO–Ag(111) potentials was found to be negligible. Hence, we shall from here on suppress the explicit dependence of the interaction potential on this angle. For both the $|+\rangle$ and $|-\rangle$ potentials, CEM calculations of the interaction energies above the atop, twofold bridge, and threefold center sites were carried out on an equispaced grid of 9 angles from $\theta = 0$ to π, and a grid of ~ 25 molecule–surface distances ranging from 2 to 10 bohr. For each value of θ, the calculated points as a function of Z were fit to the functional form

$$V_\pm(Z,\theta) = c_{1i}\exp(\beta_1 Z) + (c_{2i} + c_{3i}Z)\exp(\beta_2 Z) + c_{4i}\{\tanh[\alpha(Z - Z_0)] - 1\}/Z^6, \tag{2}$$

with coefficients given in Table I of DA.[26] Since the CEM calculations[26] do not include the electronic correlation effects which are responsible for dispersion forces, no attempt was made to force the fit to follow a Z^{-3} dependence asymptotically.

To compute the interaction potential for any location of the NO molecule above the surface, we expanded the interaction potential in terms of the reciprocal lattice basis vectors, namely,

$$V_\pm(X,Y,Z,\theta) = V_{00}^\pm(Z,\theta) + V_{10}^\pm(Z,\theta) f_{10}(X,Y) + V_{11}^\pm(Z,\theta) f_{11}(X,Y) + \text{higher order terms.} \tag{3}$$

Here

$$f_{10} = [\cos(\mathbf{K}_{10}\cdot\mathbf{R}) + \cos(\mathbf{K}_{01}\cdot\mathbf{R}) + \cos(\mathbf{K}_{0,-1}\cdot\mathbf{R})]/3 \tag{4}$$

and

$$f_{11} = [\cos(\mathbf{K}_{11}\cdot\mathbf{R}) + \cos(\mathbf{K}_{1,-2}\cdot\mathbf{R}) + \cos(\mathbf{K}_{2,-1}\cdot\mathbf{R})]/3, \tag{5}$$

where $\mathbf{R} = X\hat{x} + Y\hat{y}$ and

$$\mathbf{K}_{n,m} = n\mathbf{k}_1 + m\mathbf{k}_2, \tag{6}$$

$\mathbf{k}_1$ and $\mathbf{k}_2$ being the basis vectors of the reciprocal lattice. For a hexagonal lattice (in the coordinate system used herein), these are

$$\mathbf{k}_1 = (2\pi 2^{1/2}/a)[\hat{x} + \hat{y}/3^{1/2}], \tag{7a}$$

and

$$\mathbf{k}_2 = (2\pi 2^{1/2}/a)[\hat{x} - \hat{y}/3^{1/2}]. \tag{7b}$$

In Eq. (3) the V_{00} term is the site-averaged potential, which would be the appropriate description of the interaction potential if the Ag(111) surface were assumed to be flat. A weighted least-squares fit leads to the following relation between the three expansion terms (V_{00}, V_{10}, V_{11}) in Eq. (3) and the $V_\pm(Z,\theta)$ potentials at the three sites:[26]

$$V_{00}^\pm(Z,\theta) = [V_a^\pm(Z,\theta) + 3V_b^\pm(Z,\theta)]/4, \tag{8a}$$

$$V_{10}^\pm(Z,\theta) = [V_a^\pm(Z,\theta) - V_c^\pm(Z,\theta)]/3, \tag{8b}$$

$$V_{11}^\pm(Z,\theta) = [V_a^\pm(Z,\theta) - 9V_b^\pm(Z,\theta) + 8V_c^\pm(Z,\theta)]/12. \tag{8c}$$

Here $V_a^\pm$, $V_b^\pm$, and $V_c^\pm$ denote the potentials for approach above the atop, twofold bridge, and threefold center sites, respectively.

Irrespective of the location of the molecule over the surface unit cell, the V_- potentials, which describe the interaction of an NO molecule in which the singly filled 2π orbital is oriented along the surface normal when the molecular axis is oriented parallel to the surface, show a well 1500–2200 cm^{-1} (0.19–0.27 eV) deep, corresponding to a nearly flat NO with the N end slightly oriented toward the surface. The well region is sharply delimited in terms of orientation angle θ. The deepest well occurs for approach of the NO molecule above the atop site. By contrast, the V_+ potentials, which describe the interaction of an NO molecule in which the singly filled 2π orbital is oriented in a plane parallel to the surface when the molecular axis is oriented parallel to the surface, are much less anisotropic, with well depths roughly only 50% of those for the corresponding V_- potentials. As

an illustration, Fig. 1 displays contour plots of the site-averaged V_{00}^{+} and V_{00}^{-} potentials.

To interpolate smoothly as a function of the orientation angle, and for use in the quantum scattering studies described here, rather than work with V_{00}^{+} and V_{00}^{-}, it is more convenient to work with the equivalent potentials[7,11]

$$V_{\rm sum}(\theta,Z) \equiv \tfrac{1}{2}[V_{00}^{+}(\theta,Z) + V_{00}^{-}(\theta,Z)] \tag{9}$$

and

$$V_{\rm dif}(\theta,Z) \equiv \tfrac{1}{2}[V_{00}^{+}(\theta,Z) - V_{00}^{-}(\theta,Z)]. \tag{10}$$

We observe that $V_{\rm dif}$ vanishes at $\theta = 0°$. These two terms are then expanded as[7]

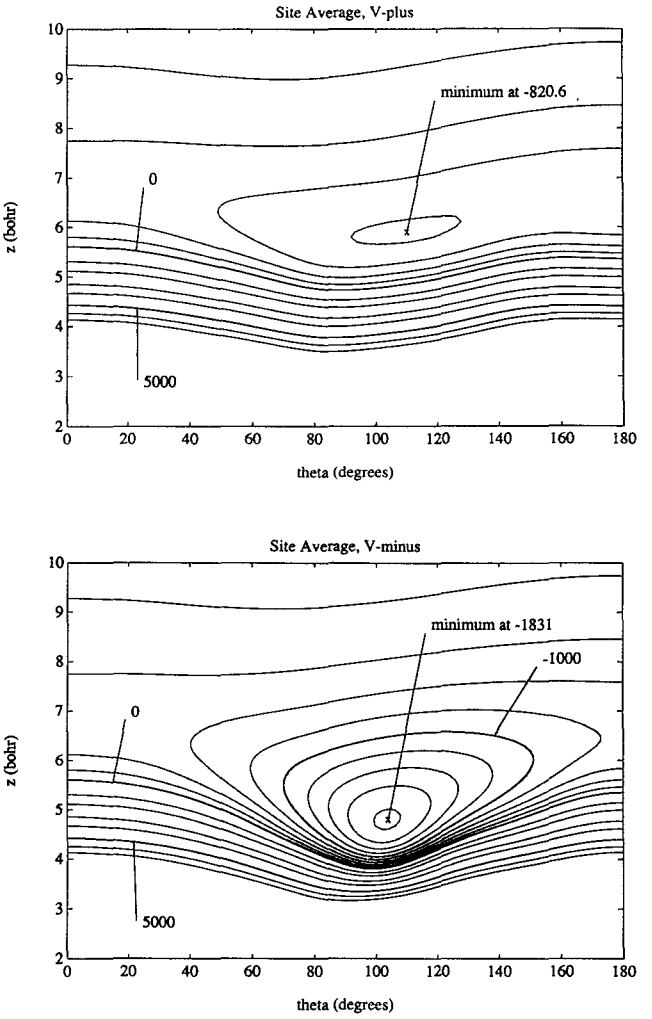

FIG. 1. (Upper panel) Site-averaged V_{00}^{+} potential [Eq. (8a)] for approach of the NO molecule above a Ag(111) surface. The V_{+} potential describes the interaction of an NO molecule in which the singly filled 2π orbital is oriented in a plane parallel to the surface when the molecular axis is oriented parallel to the surface. The negative contours designate interaction energies of $-800{:}200{:}0$ cm^{-1}; the positive contours, energies of 500, 1000, 2000, 3000, 5000, 7000, and 9000 cm^{-1}. (Lower panel) Site-averaged V_{00}^{-} potential. The V_{-} potential describes the interaction of an NO molecule in which the singly filled 2π orbital is oriented parallel to the surface normal when the molecular axis is oriented parallel to the surface. The negative contours designate interaction energies of $-1800{:}200{:}0$ cm^{-1}; the positive contours, energies of 500, 1000, 2000, 3000, 5000, 7000, and 9000 cm^{-1}.

$$V_{\rm sum}(\theta,Z) = \sum_{\lambda=0}^{8} V_{\lambda 0}(Z) d_{00}^{\lambda}(\theta) \tag{11}$$

and

$$V_{\rm dif}(\theta,Z) = \sum_{\lambda=2}^{8} V_{\lambda 2}(Z) d_{0,-2}^{\lambda}(\theta), \tag{12}$$

where $d_{m,n}^{\lambda}$ is a reduced rotation matrix element.[32,33]

III. SCATTERING DYNAMICS

The electronic-rotational wave functions of the NO molecule can be expressed in an intermediate coupling basis as[34,35]

$$|JMF_1\epsilon\rangle = \cos\theta_J |JM,\Omega=\tfrac{1}{2},\epsilon\rangle + \sin\theta_J |JM,\Omega=\tfrac{3}{2},\epsilon\rangle, \tag{13}$$

$$|JMF_1\epsilon\rangle = -\sin\theta_J |JM,\Omega=\tfrac{1}{2},\epsilon\rangle + \cos\theta_J |JM,\Omega=\tfrac{3}{2},\epsilon\rangle, \tag{14}$$

where the pure Hund's case (a) wave functions are denoted by $|JM\Omega\epsilon\rangle$ with symmetry index $\epsilon = +1$ and $\epsilon = -1$ for, respectively, the e and f labeled Λ-doublet states.[36] Here J is the total angular momentum of the NO molecule with space- and molecule-frame projections of M and Ω. The F_1 and F_2 labels designate the lower and higher (in energy) of the two spin–orbit manifolds. The mixing angle θ_J in Eqs. (13) and (14) is obtained by diagonalization of a 2×2 molecular Hamiltonian.[37,38] For NO at low J, in the pure case (a) limit, θ_J approaches 0. As J increases, and the rotational spacing becomes large compared to the spin–orbit splitting [$A_{\rm so} = 119.8$ cm^{-1} (Ref. 39)], the case (b) limit is approached, and θ_J approaches $\pi/2$. For NO, the mixing between the case (a) states becomes significant for $J \gtrsim 20$–30.[11] In the present paper we treat the scattering as that of a rigid rotor, explicitly ignoring vibrationally inelastic effects. For future reference, we plot in Fig. 2 as a function of J the splitting between the two Λ-doublets in both the F_1 and F_2 manifolds, and also, the splitting between the F_1 and F_2 spin–orbit manifolds.

Within the assumption of a flat, rigid surface, the wave function of the NO molecule as it approaches the surface can be written as

$$\Psi(Z) = \sum_{JM'F_i'\epsilon'} C_{J'M'F_i'\epsilon'}(Z) |J'M'F_i'\epsilon'\rangle. \tag{15}$$

The expansion coefficients satisfy the usual close-coupled (CC) equations for scattering of a molecule from an uncorrugated surface.[40–42] The solution to these CC equations must satisfy the boundary conditions[7,8,40]

$$\sum_{Z\to\infty} C_{J'M'F_i'\epsilon'}(Z) = \delta_{JJ'}\delta_{MM'}\delta_{\epsilon\epsilon'}\delta_{F_iF_i'} \exp(-ik_{J'F_i'\epsilon'}Z) + (k_{JF_i\epsilon}/k_{J'F_i'\epsilon'})^{1/2} S_{J'M'F_i'\epsilon',JMF_i\epsilon} \times \exp(ik_{JF_i\epsilon}Z). \tag{16}$$

Here the wave vectors are defined by

$$k_{JF_i\epsilon} = \hbar^{-1}[2m(E - E_{JF_i\epsilon})]^{1/2}, \tag{17}$$

where E is the total energy, m is the mass of the NO molecule, and $E_{JF_i\epsilon}$ is the internal energy of the $|JMF_i\epsilon\rangle$ state.

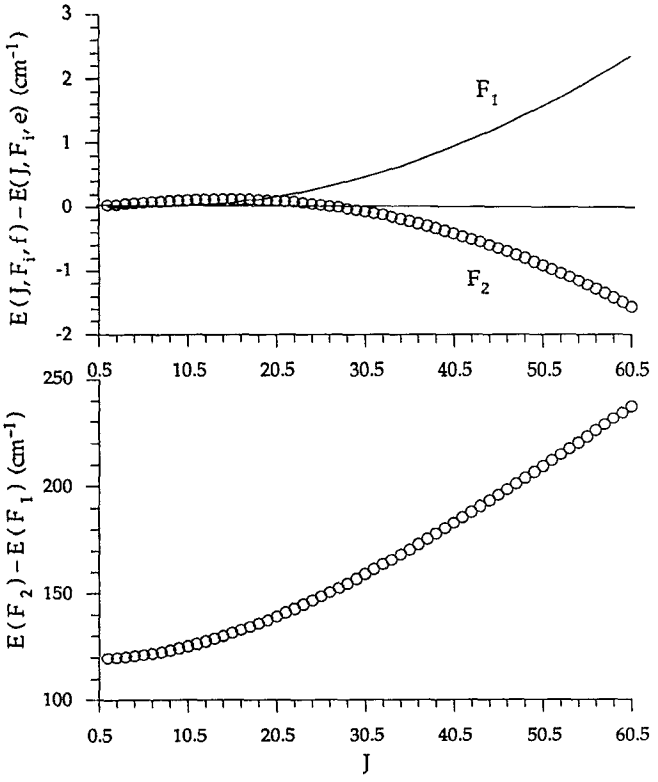

FIG. 2. (Upper panel) Energy splitting in cm^{-1} between the f and e Λ-doublet levels of both the F_1 and F_2 spin–orbit manifolds of NO as a function of the rotational quantum number. (Lower panel) Energy splitting in cm^{-1} between the f Λ-doublet levels of the F_1 and F_2 spin–orbit manifolds of NO as a function of the rotational quantum number. Since the splitting between the two Λ-doublet levels of a particular spin–orbit manifold is so small (upper panel), on the scale of the lower panel the splitting between the e Λ-doublet levels of the F_1 and F_2 spin–orbit manifolds (not shown) is identical to the displayed splitting between the f Λ-doublet levels.

The probability of a $J'M'F_i'\epsilon' \rightarrow JMF_i\epsilon$ transition can be written as

$$P_{J'M'F_i'\epsilon' \rightarrow JMF_i\epsilon} = |S_{J'M'F_i'\epsilon', JMF_i\epsilon}|^2. \quad (18)$$

Full CC calculations were carried out using the site-averaged (flat surface) potentials of DA [Fig. 1, $V_{00}^{\pm}$ in Eq. (3)]. The total energy used was 6900 cm^{-1} (0.8555 eV). To simulate the finite spread of translational energies in a real beam, calculations were carried out at 9 different total energies ranging from 6600 to 7200 cm^{-1}. The calculated transition probabilities were then "averaged" by weighing each energy by an assumed Gaussian distribution centered at 6900 cm^{-1} and with a FWHM of 345 cm^{-1}. In other words

$$\langle P_{i \rightarrow f} \rangle = \sum_{n=1}^{9} P_{i \rightarrow f}(E_n) f(E_n) \Big/ \sum_{n=1}^{9} f(E_n), \quad (19)$$

where $f(E_n) = \exp[-\alpha(E_n - E_j - 6900)^2]$ with $\alpha = 2.3294 \times 10^{-5}$ cm, and $E_n = 6600{:}75{:}7200\ cm^{-1}$.

At a total energy of 6900 cm^{-1} all rotational energy levels up to $J = 64.5$ in the $\Omega = \frac{1}{2}$ manifold and all energy levels up to $J = 63.5$ in the $\Omega = \frac{3}{2}$ manifold are energetically accessible (open). Due to the depth of the potential well in the V_- potential surface, it was necessary to include in the rotational basis all levels with $J \leqslant 72.5$ to obtain convergence in the transition probabilities. For collisions with an uncorrugated surface, the CC equations are diagonal in M, the projection of the molecular angular momentum along the surface normal. The total dimensionality of the CC equations is then $4J_{max}$. This implies a total of 288 coupled channels. To average over all initial values of M in an unpolarized initial beam of NO, CC calculations must be repeated for all values of $\frac{1}{2} \leqslant M \leqslant \max(J_i)$, where $\max(J_i)$ is the maximum rotational level with substantial population in the initial beam. Here we took $\max(J_i)$ to be 5.5.

In any experiment involving a molecular beam striking a surface, the observed scattering into a given final rotational level is the sum of the transition probabilities into that level from all initial states present in the beam, weighted by their relative populations in the incident beam. Thus we can write

$$P_{JF_i\epsilon} = \sum_{J'M'F_i'\epsilon'} \delta_{MM'} \rho_{J'M'F_i'\epsilon'} P_{J'M'F_i'\epsilon' \rightarrow JMF_i\epsilon}, \quad (20)$$

where $\rho_{J'M'F_i'\epsilon'}$ designates the relative population of the $J'M'F_i'\epsilon'$ level in the incoming beam. The Kroenecker delta in Eq. (20) reflects the fact that a smooth surface cannot induce changes in the magnetic quantum number.[41] We shall assume that the population of the initial beam is confined to the $\Omega = \frac{1}{2}$ spin–orbit manifold and, further, that the rotational distribution can be characterized by a temperature T_{rot}, so that

$$\rho_{J'M'F_i'\epsilon'} = \delta_{F_i',1} \exp(-E_{J'F_i'\epsilon'}/kT_{rot})/Q_{rot}. \quad (21)$$

Here Q_{rot} is the rotational partition function at temperature T_{rot}.

The CC equations were solved using the Hibridon scattering package.[43] The calculations were carried out on an FPS-M64 at the University of Maryland, Center for Intensive Computation. On this machine with a LINPACK benchmark of 2.1 MFlop,[44] for one value of M solution of the 288 CC equations took 30 min of cpu time at a first energy and 15 min at each subsequent energy.

IV. RESULTS: TRANSITION PROBABILITIES SUMMED AND AVERAGED OVER FINE-STRUCTURE LEVELS

By summing the calculated transition probabilities over the four final states with a given J (two Λ-doublets and two spin–orbit manifolds), and then averaging over the four initial states with a given J, one obtains averaged transition probabilities which one might suppose, at first thought, could be compared directly with the rotationally inelastic $J' \rightarrow J$ transition probabilities which one would measure in collision experiments involving a closed-shell molecule in a $^1\Sigma$ electronic state. The $^2\Pi$ transition probabilities, summed and averaged over fine-structure level, are displayed in Fig. 3. In Fig. 4 the log of the transition probability, divided by the rotational degeneracy of the final state, is plotted against the average rotational energy $[BJ(J+1)]$ of the final state. We observe first that the results averaged over a 5% FWHM Gaussian distribution of translational energies centered at $E = 6900\ cm^{-1}$ [Eq. (19), solid curve in the upper panel] differ insignificantly from the results obtained from a single calculation at $E = 6900\ cm^{-1}$. This was found to be true

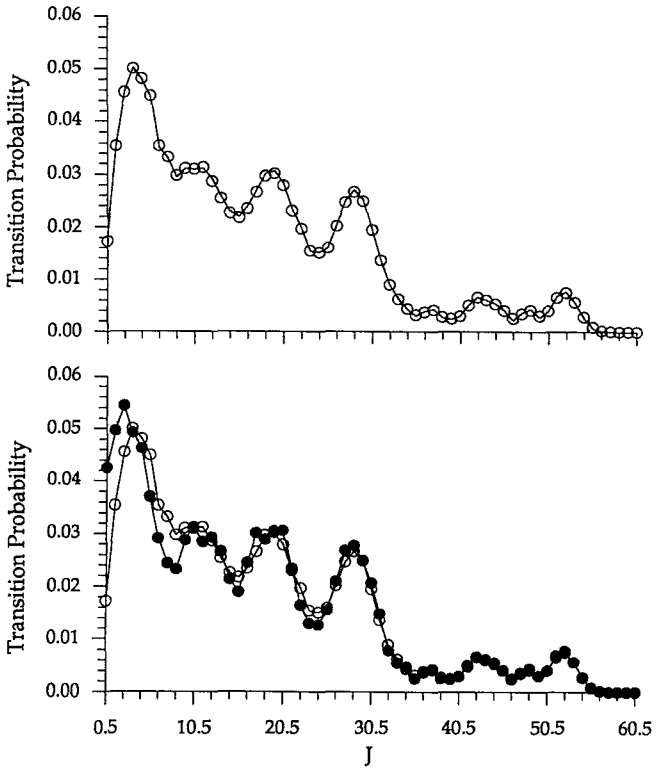

FIG. 3. Rotationally inelastic NO–Ag(111) transition probabilities out of the $\Omega = \frac{1}{2}$ spin–orbit manifold, summed over final state Λ-doublet and spin–orbit levels, and averaged over initial state Λ-doublet levels. Results plotted against the rotational angular momentum of the final state. (Upper panel) The plain solid curve designates calculations at a singlet total energy of 6900 cm^{-1}; the open circles are the results of averaging over a Gaussian distribution in initial translational energy [Eq. (19)]. In both cases the distribution of initial rotational states was characterized by a rotational temperature of 50 K. (Lower panel) Results again averaged over a Gaussian distribution in initial translational energy centered at $E = 6900\ cm^{-1}$, but with two different assumed rotational temperatures of the initial beam. The open circles (identical to the open circles in the upper panel) corresponds to $T_{rot} = 50$ K, while the filled circles correspond to $T_{rot} = 10$ K.

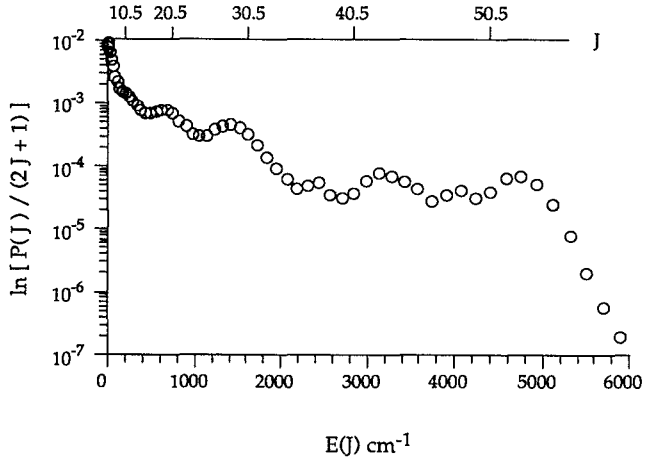

FIG. 4. Rotationally inelastic NO–Ag(111) transition probabilities out of the $\Omega = \frac{1}{2}$ spin–orbit manifold, summed over final state Λ-doublet and spin–orbit levels, and averaged over initial state Λ-doublet levels. These transition probabilities, divided by the final state rotational degeneracy, are plotted against the average rotational energy of the final state. The plotted points (equivalent to the open circles in the upper panel of Fig. 3) correspond to the results of averaging over a Gaussian distribution in initial translational energy centered at $E = 6900\ cm^{-1}$, with an assumed rotational temperature of $T_{rot} = 50$ K.

even for the more highly state-resolved transition probabilities (to be discussed below).

The interference pattern seen in the upper panel of Fig. 3 is evidence of three (and perhaps more) "rotational rainbows,"[1,45] at $J \cong 2.5$, $J \cong 28.5$, and at $J \cong 52.5$. Additional supernumerary oscillations can be observed on the bright (low J) side of each primary rainbow. As can be seen in the lower panel of Fig. 3, the rainbow structure is smoothed somewhat by the averaging due to the presence of several rotational levels in the initial beam. This effect becomes more marked as the rotational temperature associated with the initial rotational distribution increases.

As mentioned in Sec. I, in most prior theoretical work the dynamics has been described in terms of only one PES,[1-6,9,10,13-15,19] with the implicit assumption that rotational level structure of the NO molecule could be treated as if it were in a $^1\Sigma$ electronic state, without the complications associated with spin–orbit and Λ-doublet splitting. One necessary condition for this to be true is that the difference between the V_+ and V_- potentials be small, in other words that V_{dif} [Eq. (12)] be small compared to V_{sum} [Eq. (11)]. Although this condition may apply to the potential of Smedley and co-workers,[11] we see from Fig. 1 that it is hardly the case for the new DA potential. If there exists a sizeable difference between V_+ and V_-, then the scattering on the average potential (V_{sum}) will not necessarily be equal to the average of the transition probabilities computed from considering, sequentially, scattering on the V_+ and V_- potentials. In addition, the correct treatment of the scattering of a $^2\Pi$ molecule, used here, inescapably allows interference between the two PES as the collision occurs. Thus there is no *a priori* reason to expect that the resulting transition probabilities, even if summed and averaged over fine-structure levels, will be identical to those predicted by treating the NO molecule as a $^1\Sigma$ diatomic and averaging the transition probabilities for scattering on the V_+ and V_- PES.

To investigate this issue we show in Fig. 5 transition probabilities determined by treating the NO molecule as a $^1\Sigma$ diatomic. We see that the rotational distributions are very different depending on whether V_+, V_-, or V_{sum} is used to describe the interaction potential. The scattering from all three potentials displays both high- and low-J rainbows. On more closer examination of the upper panel of Fig. 3, and comparison with Fig. 5, we see that the fine-structure summed $^2\Pi$ transition probabilities show clearly the presence of two pairs of rotational rainbows, one from scattering on the V_+ PES and the other from scattering on the V_- PES.

Notwithstanding the residual presence of these rotational rainbows, the rotational distribution arising from scattering on just the average potential (plain solid curve in the upper panel of Fig. 5) is dramatically different from the fine structure summed $^2\Pi$ transition probabilities (upper panel, Fig. 3). This implies that it is qualitatively incorrect to simulate the scattering of NO from a Ag(111) surface by a

single potential energy surface, even if one is not interested in the fine-structure dependence of the inelastic scattering.

The lower panel of Fig. 5 compares the fine structure summed $^2\Pi$ transition probabilities with the *average* of the $^1\Sigma$ transition probabilities for scattering on both the V_+ and V_- PES. The difference between these two curves is the reflection of quantum interference between the two PES, which occurs in the correct treatment of the scattering, since any single "trajectory" actually samples both PES. It is the amplitude, rather than the period, of the rainbow oscillations which appears to be most sensitive to this quantum interference. Overall, though, the average of the $^1\Sigma$ rotational distributions for scattering on the two PES (V_+ and V_-) provides a much better description of the true rotational distribution than the calculation based on a *single* potential surface which is the average of V_+ and V_-.

V. RESULTS: TRANSITION PROBABILITIES INTO DIFFERENT SPIN–ORBIT MANIFOLDS

In the experiments of Auerbach[21] and Zare,[22] the populations in the impinging supersonic NO beams were confined

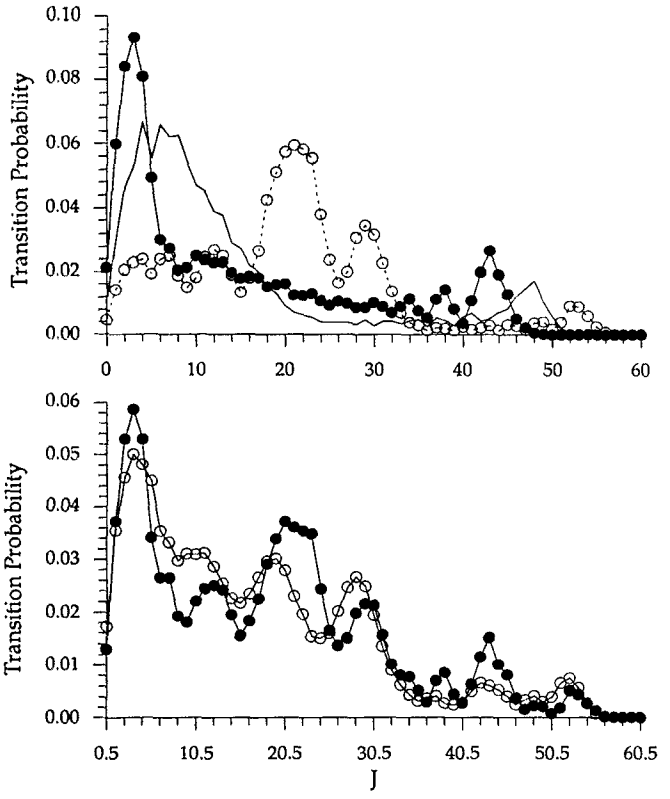

FIG. 5. (Upper panel) Rotationally inelastic NO–Ag(111) transition probabilities determined by treating the molecule as a $^1\Sigma$ diatomic; $\langle E\rangle = 6900\,\mathrm{cm}^{-1}$, $T_{rot} = 50$ K. The solid curve refers to scattering on the average potential V_{sum}; the filled circles, to scattering on V_{00}^{+}; and the open circles, connected by a dashed curve, to scattering on V_{00}^{-}. (Lower panel) The open circles (identical to the open circles in the two panels in Fig. 3) represent the correct $^2\Pi$ transition probabilities out of the $\Omega = \frac{1}{2}$ spin–orbit manifold, summed over final state Λ-doublet and spin–orbit levels, and averaged over initial state Λ-doublet levels, from the lower panel of Fig. 3. The filled circles designate the average of the rotational distributions from scattering separately on the V_{00}^{+} and V_{00}^{-} PES and treating the molecule as a $^1\Sigma$ diatomic (the average of the filled and open circles in the upper panel).

primarily to the lower (F_1) spin–orbit manifold. In the case (a) limit the F_1 and F_2 manifolds can be characterized by definite values of Ω ($\Omega = \frac{1}{2}$ for F_1 and $\Omega = \frac{3}{2}$ for F_2). As discussed in Sec. III, as J increases, the $\Omega = \frac{1}{2}$ and $\Omega = \frac{3}{2}$ wave functions become increasingly mixed, and, for a given value of J, the splitting between the F_1 and F_2 levels increases quadratically.

With resolution of the F_i label of the final rotational level, one can compare the scattering into the two spin–orbit manifolds, as a function of J, namely,

$$P_{JF_i} = \sum_{\epsilon} P_{JF_i\epsilon}, \tag{22}$$

where the transition probabilities $P_{JF_i\epsilon}$ are defined by Eq. (21). Since, for a given value of J, the degeneracy of the F_1 and F_2 levels is identical, one would expect from a statistical model that the ratio of the transition probability into the lower (F_1) spin–orbit manifold would always be larger than the transition probability for scattering into the upper (F_2) spin–orbit manifold. In a simplistic model the ratio of these transition probabilities would be $\exp(-A_{so}/kT_{so})$, where T_{so} is some effective final-state spin–orbit "temperature." In fact, since the splitting between the F_1 and F_2 levels of a given J increases quadratically as J increases (Fig. 2), energy gap arguments would predict that the ratio of these transition probabilities should actually *decrease* below that predicted by the exponential in the preceding sentence.

However, within the energy sudden limit,[7,8,12] if one sums over the final state Λ-doublet levels, the transition probability for scattering from a low-J level into a high-J F_1 level is, in fact, predicted to be *equal* to the transition probability for scattering into a high-J F_2 level.[7] In other words, in the energy sudden limit, the final state spin–orbit temperature T_{so}, should be infinite. The physical origin of this F to F_2 equality involves quantum mechanical interference between scattering on the V_+ and V_- potential energy surfaces, mediated by the mixing between the case (a) electronic wave functions,[7] which becomes stronger and stronger as J increases (see Sec. III and Fig. 1 of Ref. 11).

In light of this prediction, we here examine the scattering into rotational levels of the F_1 and F_2 spin–orbit manifolds as predicted by our close-coupling calculations based on the potential energy surfaces of DA.[26] These are shown in Fig. 6. We observe that for $J' \leqslant 30.5$, transitions are more probable within the spin–orbit manifold initially populated (F_1 here). At low J, where a case (a) limit is appropriate, transitions *within* a particular spin–orbit manifold are induced by the V_{sum} term in the potential, while transitions *between* the $\Omega = 1/2$ and $\Omega = 3/2$ manifolds are induced by the V_{dif} term.[7,11] Since the magnitude and anisotropy in V_{sum} will be larger than for V_{dif}, we anticipate that the probabilities for $F_1 \rightarrow F_1$ transitions will be larger than for $F_1 \rightarrow F_2$ transitions. This tendency will be further reinforced by the fact that for a given upward $J' \rightarrow J$ transition with $J > J'$ the energy gap for $F_1 \rightarrow F_2$ transitions increases with J (Fig. 2).

As the final state rotational angular momentum increases beyond 30.5, the magnitude of the $F_1 \rightarrow F_1$ and $F_1 \rightarrow F_2$ transition probabilities for a given final state J becomes nearly identical, despite the increasing energy gap

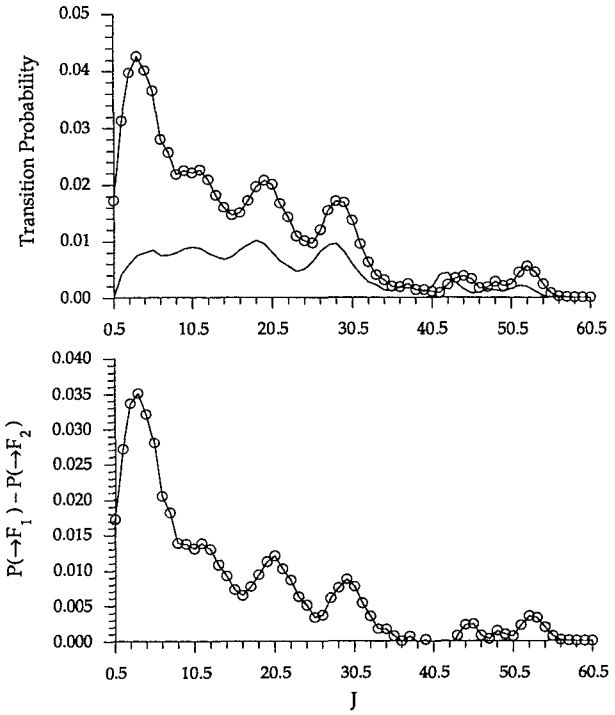

FIG. 6. Rotationally inelastic NO–Ag(111) transition probabilities out of the $\Omega = \frac{1}{2}$ spin–orbit manifold, summed over final state Λ-doublet levels, and averaged over initial state Λ-doublet levels; $\langle E \rangle = 6900\ \mathrm{cm}^{-1}$, $T_{\mathrm{rot}} = 50$ K. The distribution of initial rotational states was characterized by a rotational temperature of 50 K. (Upper panel) The open circles represent scattering into rotational levels of the lower (F_1) spin–orbit manifold, while the plain solid curve represents scattering into rotational levels of the upper (F_2) spin–orbit manifold. (Lower panel) The difference between the transition probabilities for scattering into the lower (F_1) and upper (F_2) spin–orbit manifolds (the difference between the two curves in the upper panel).

(Fig. 2). For $J \geqslant 30.5$, the final rotational state approaches Hund's case (b), while the initial state remains case (a). As anticipated,[7] for these low J, case (a) → high J, case (b) transitions, the pronounced propensity for scattering into the same spin–orbit manifold disappears.

VI. RESULTS: TRANSITION PROBABILITIES INTO SYMMETRIC VS ANTISYMMETRIC Λ-DOUBLET LEVELS

In the experiments of Auerbach[21] and Zare,[22] in the initial NO beam the Λ-doublet levels of the molecule are not selected, so that both the e and f states[36] will be present with equal probability, for a given value of J and Ω. With spectroscopic detection, one can compare the scattering from these low J Λ-doublets, which are equally populated, into one or the other of the high J Λ-doublet levels. For a $^2\Pi$ molecule in the case (b) limit the wave functions for the $e(\epsilon = 1)$ levels in the F_1 manifold and the $f(\epsilon = -1)$ levels in the F_2 manifold are *symmetric* with respect to reflection in the plane of rotation of the molecule [$\Pi(A')$] while the wave functions for the f levels in the F_1 manifold and the e levels in the F_2 manifold are *antisymmetric* with respect to reflection [$\Pi(A'')$].[35,46]

In the energy sudden limit the transition probabilities for scattering from a low-J level into the symmetric Λ-doublet levels of a high-J state will not necessarily be equal to those for scattering into the antisymmetric Λ-doublet levels of the same high-J state.[7] This selection of one Λ-doublet level over another would be unexpected, at least on statistical grounds, since the splitting between the e and f Λ-doublet levels is always negligibly small (see Fig. 2) compared to the total collision energy in typical experiments (2000–7000 cm^{-1}). In the sudden limit the mixing between the transition amplitudes associated with scattering on the V_+ and V_- surfaces occurs with one sign (positive or negative) in the case of transitions into the $\Pi(A')$ Λ-doublet levels but with the opposite sign for transitions into the antisymmetric [$\Pi(A'')$] Λ-doublet levels. This constructive or destructive interference becomes enhanced with increasing J, as the final state approaches the case (b) limit [$\theta_J = \pi/4$ in Eqs. (13) and (14)]. For transitions between low J levels, which can be well described in Hund's case (a), the scattering will be *independent* of the final state Λ-doublet level, provided that the Λ-doublet levels of the initial state are populated equally.

Similar Λ-doublet propensities[47] in gas-phase collisions of $^2\Pi$ molecules in Hund's case (b) have been interpreted by Dagdigian and co-workers.[48] There the propensity toward preferential population of the $\Pi(A')$ or $\Pi(A'')$ levels could be predicted from the sign of the leading terms in the expansion of the difference potential [Eq. (12)].

To investigate the possible propensity toward population of either the symmetric or antisymmetric Λ-doublet levels in collisions of NO with a Ag(111) surface, in the upper panel of Fig. 7 we have plotted separately the transition probability for scattering into Λ-douplet levels of A' and A'' reflection symmetry, namely

$$P_{J\epsilon'} = \sum_{F_i} P_{JF_i\epsilon'}. \tag{23}$$

The plotted transition probabilities are summed over final spin–orbit state. As anticipated, at low J, where both the initial and final rotational states are well described in Hund's case (a), there is no preference for scattering into either one or the other Λ-doublet level. At higher J there emerges a definite preference for scattering into levels of A'' reflection symmetry. This preference is maintained for all J, except for a small region near $J = 40.5$. An additional view into this Λ-doublet propensity is provided by the lower panel of Fig. 7, in which we plot the *polarization* of the final state Λ-doublet distribution, namely

$$A(J) = [P_J(A'') - P_J(A')]/[P_J(A'') + P_J(A')], \tag{24}$$

where $P_J(A'')$ is the probability for scattering into levels of A'' symmetry ($F_1 f$ and $F_2 e$) and $P_J(A')$ is the probability for scattering into levels of A' symmetry ($F_1 e$ and $F_2 f$).[46]

It is intriguing to observe that the preferential population of the A'' levels is strongest for final J states that correspond to the rotational rainbows associated with the V_- potential ($J = 20.5, 30.5, 52.5$; see the dot–dash curve in the upper panel of Fig. 5). In the interpretation by Dagdigian and co-workers[48] of Λ-doublet propensities in gas-phase $^2\Pi$ molecules, preferential population of either the $\Pi(A')$ or $\Pi(A'')$ levels was related to the magnitude of the coupling

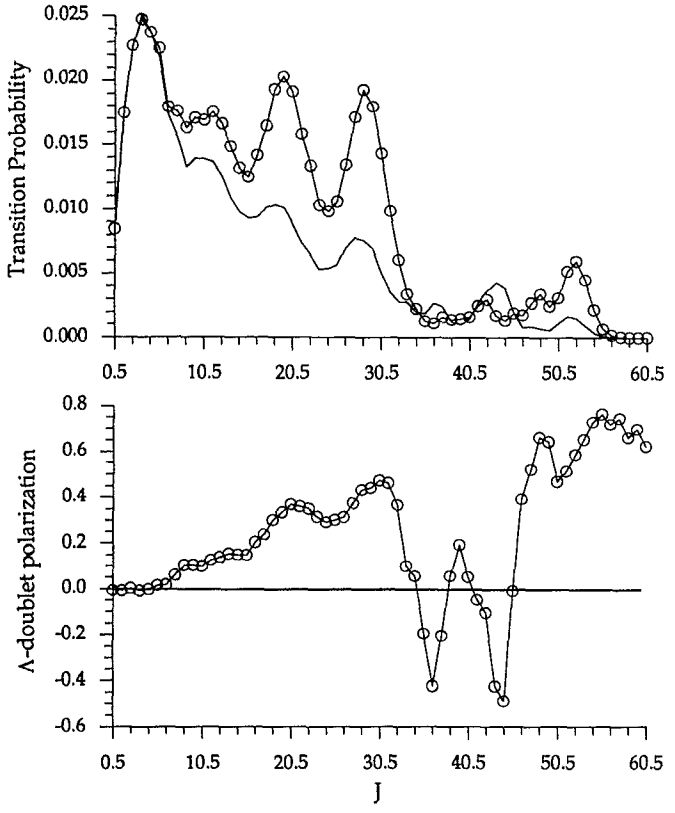

FIG. 7. (Upper panel) Rotationally inelastic NO–Ag(111) transition probabilities, summed over final state spin–orbit manifold, but resolved in final state Λ-doublet levels; $\langle E \rangle = 6900\,\mathrm{cm}^{-1}$, $T_{\mathrm{rot}} = 50$ K. The plain solid curve represents scattering into Λ-doublet levels of A'' reflection symmetry, while the curve with open circles represents scattering into Λ-doublet levels of A' reflection symmetry. (Lower panel) Polarization of the Λ-doublet transition probabilities, summed over final state spin–orbit manifold, defined by Eq. (24).

matrix element between the initial and final states. Here such an analysis is not possible, since the interaction potential used, which involves Legendre expansion terms only up to order 8 [Eqs. (11) and (12)], will not directly couple the low J states present in the initial beam ($J \leqslant 5.5$) with the high J states ($J \geqslant 15.5$) at which the strongest Λ-doublet propensities are seen (Fig. 7).

VII. VARIATION WITH SURFACE SITE

With the expansion of the NO–Ag(111) potential given in Eq. (3) it is, in principle, possible to determine the effect of surface corrugation on the scattering of the NO molecule. To do so would require expanding the scattering wave function not just in terms of the rotational–electronic states of the NO molecule [Eq. (15)] but as a product of NO rotational–electronic states multiplied by diffraction states.[49] Since the mass of NO is high, many diffraction states will be populated, so that the total number of internal states would become rapidly too large to treat by time-independent close-coupling techniques (although this might be possible using wave-packet close-coupling techniques[17,18,50,51]). Nevertheless, some insight can be gained by carrying out scattering calculations identical to those described in Sec. III, but using, instead of the surface averaged PES [$V_{00}^{\pm}(Z,\theta)$ in Eq. (3)], the three sets of PES, $V_a^{\pm}(Z,\theta)$, $V_b^{\pm}(Z,\theta)$, and $V_c^{\pm}(Z,\theta)$, which describe the interaction when an NO molecule approaches above the atop, twofold bridge, and threefold center sites.[26]

The upper panel of Fig. 8 shows the transition probabilities, averaged over the initial state fine-structure level and summed over the final-state find-structure level, for approach over the three sites. We observe, as might have been anticipated, considerable variation in the position and magnitude of the rainbow oscillations. This is particularly apparent in the region ($10.5 < J < 30.5$) corresponding to the strong rainbow arising from scattering on the V_- potential (see the upper panel of Fig. 5). Despite the qualitative similarity between the V_a, V_b, and V_c potentials,[26] we observe that the oscillatory features in the final state rotational distributions appear to be very sensitive to subtle differences between these potentials.

In order to simulate scattering from the entire surface, it might be reasonable to average the three sets of transition probabilities arising from scattering on the $V_a^{\pm}$, $V_b^{\pm}$, and $V_c^{\pm}$ PES, in a way identical to the least-squares averaging of

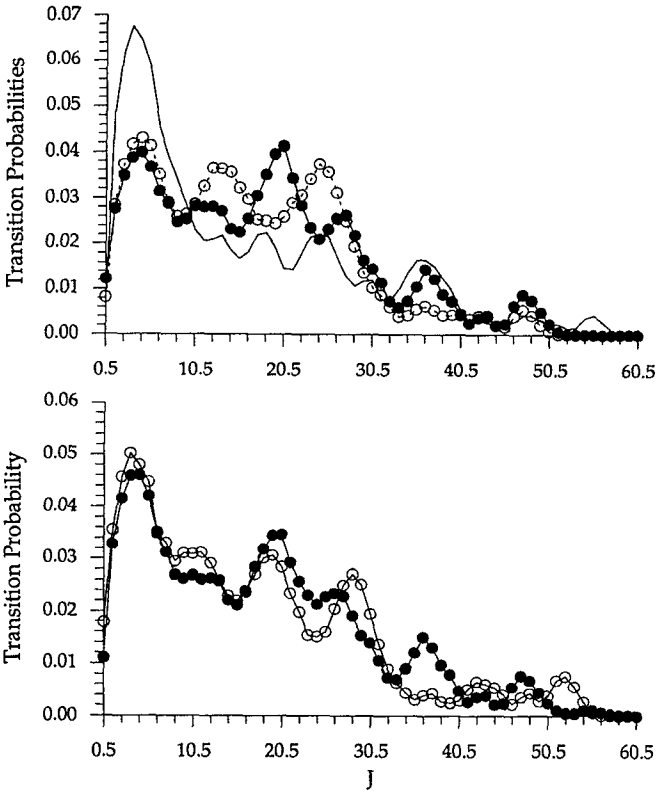

FIG. 8. Rotationally inelastic NO–Ag(111) transition probabilities out of the $\Omega = \frac{1}{2}$ spin–orbit manifold, summed over final state Λ-doublet levels, and averaged over initial state Λ-doublet levels; $\langle E \rangle = 6900\,\mathrm{cm}^{-1}$. $T_{\mathrm{rot}} = 50$ K. (Upper panel) Results for scattering on the atop potential (plain solid curve), on the twofold bridge potential (solid circles), and on the threefold center potential (open circles connected by dashed curve). (Lower panel) Comparison of the site average of these fine-structure averaged transition probabilities (filled circles) with the corresponding fine-structure-averaged transition probabilities (open circles) obtained by scattering on the site-averaged potential. The latter curve is identical to that marked by open circles in the upper panel of Fig. 3.

the potential contained in Eq. (8a). We would then define site-averaged transition probabilities by

$$\langle P_{JF_i\epsilon}\rangle = \left[P^a_{JF_i\epsilon} + 3P^b_{JF_i\epsilon}\right]/4. \tag{25}$$

These are displayed, again summed and averaged over fine-structure level, in the lower panel of Fig. 8, and compared with the corresponding transition probabilities for the site-averaged PES, $V^{\pm}_{00}$. The similarity between these two curves is high, although some noticeable differences persist, primarily in the region of the high J oscillations.

The propensity for scattering into the lower F_1 spin–orbit manifold can be also compared by determination of the site-averaged transition probabilities analogous to Eq. (22), namely

$$\langle P_{JF_i}\rangle = \sum_{\epsilon} \langle P_{JF_i\epsilon}\rangle. \tag{26}$$

These are plotted in the upper panel of Fig. 9. These should be compared with the equivalent transition probabilities for scattering off the site-averaged potential (upper panel of Fig. 6). Despite some differences in the relative magnitude of the transition probabilities, we still observe a strong preference for scattering into the lower spin–orbit manifold at low J, and the disappearance of this preference as the final states become described in Hund's case (b) ($J \gtrsim 30.5$).

Finally, we examine the effect of surface averaging on the propensity for scattering into the A'' Λ-doublet levels. Here, in analogy with Eqs. (24) and (26) we define the site-averaged transition probabilities

$$\langle P_{J\epsilon}\rangle = \sum_{F_i} \langle P_{JF_i\epsilon}\rangle. \tag{27}$$

These are plotted in the lower panel of Fig. 9. We observe that the preference toward population of the $\Pi(A'')$ Λ-doublet levels is not at all diminished by averaging over the symmetry sites of the unit cell.

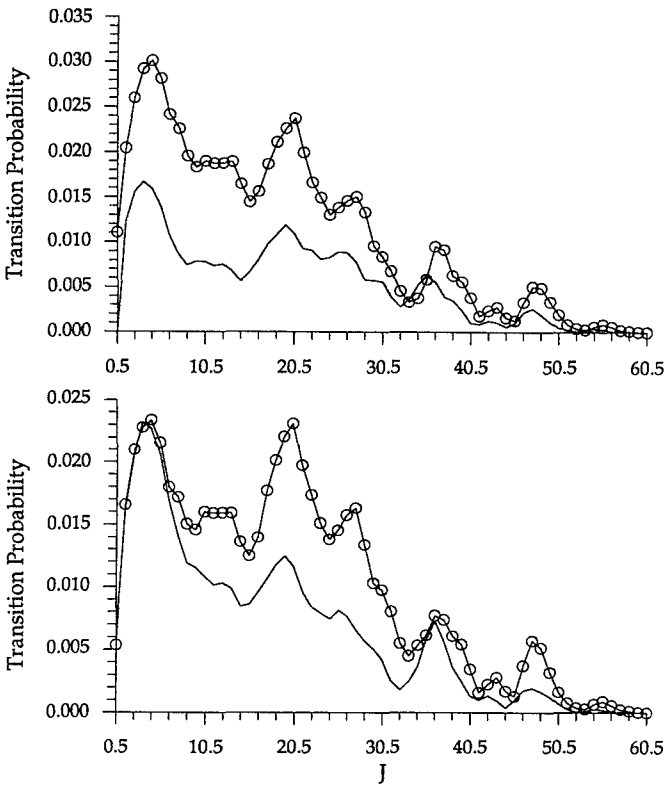

FIG. 9. In both panels the results shown are the site average of transition probabilities for scattering on the atop, twofold bridge, and threefold center site potentials. (Upper panel) Rotationally inelastic NO–Ag(111) transition probabilities out of the $\Omega = \frac{1}{2}$ spin–orbit manifold, summed over final state Λ-doublet levels, and averaged over initial state Λ-doublet levels; $\langle E\rangle = 6900\,\mathrm{cm}^{-1}$, $T_{\mathrm{rot}} = 50$ K. The open circles represent scattering into rotational levels of the lower (F_1) spin–orbit manifold, while the plain solid curve represents scattering into rotational levels of the upper (F_2) spin–orbit manifold. This figure should be compared with the upper panel of Fig. 6. (Lower panel) Rotationally inelastic NO–Ag(111) transition probabilities, summed over final state spin–orbit manifold, but resolved in final state Λ-doublet levels; $\langle E\rangle = 6900\,\mathrm{cm}^{-1}$, $T_{\mathrm{rot}} = 50$ K. The displayed transition probabilities are the site averaged of transition probabilities corresponding to scattering off the atop, bridge, and center site PES. The open circles represent scattering into Λ-doublet levels of A'' reflection symmetry, while the *plain solid* curve represents scattering into Λ-doublet levels of A' reflection symmetry. This figure should be compared with the upper panel of Fig. 7.

VIII. COMPARISON WITH PREVIOUS WORK

Although there have been many theoretical studies of collisions of NO with the (111) face of a Ag crystal,[1–19] the only prior studies which properly take into account the open-shell character of the NO molecule and the concommitant dual potential surface aspect of the interaction are those of Alexander, Corey, and co-workers.[11–13,16–18] There exist three major qualitative differences between the PES used here and those used by these authors:[11,26] First, the minima in the present V_+ and V_- potentials both correspond to the NO molecule strongly tilted with respect to the surface normal, while in the PES of Smedley *et al.* a perpendicular orientation with the N end down is preferred. Secondly the well depth in the PES of Smedley *et al.* is more than twice as large as in the present potentials. Finally, the difference between the V_+ and V_- potentials used by Smedley *et al.* is qualitatively and quantitatively much smaller than in the case of the present PES.[26] The major similarity between the two sets of PES is that in both cases the V_- potentials are predicted to be more strongly binding.

Notwithstanding these differences, we observe, comparing Fig. 3 of the present paper with Fig. 5 of Ref. 11, that the final state rotational distributions, summed and averaged over fine-structure level, reported by Smedley *et al.* at a collision energy of 6700 cm^{-1} are quite similar to those determined here, particularly in the case of the potential labeled IV by Smedley *et al.* Our calculations show a much clearer tendency for preferential scattering into the lower spin–orbit manifold, F_1, at low J with a tendency for equal populations of both spin–orbit manifolds at higher J, than do the calculations of Smedley *et al.* (Fig. 8 of Ref. 11). A similar observation applies to the probabilities for scattering into the $\Pi(A'')$ as opposed to $\Pi(A')$ Λ-doublet levels: Smedley *et al.* do not report a clear preference here, except in the case of their potential II where the $\Pi(A')$ Λ-doublet levels are strongly preferred for final J levels lying near the highest rotational rainbow (Fig. 7 of Ref. 11). However, we observe here a marked preference for population of the $\Pi(A'')$ levels for virtually all final J.

The most detailed comparison with experiment is with the results of Auerbach and co-workers,[21,52] who carried out

scattering studies for an incident NO beam with normal kinetic energy of 6500 cm^{-1}. The observed rotational distributions at this energy indicate that the rotational rainbow at highest J occurs for $J \approx 38.5$, substantially less than our prediction (Figs. 3 and 8) that significant rotational excitation will occur out to $J \approx 50.5$. Experimentally, there is evidence[21] that the relative population in the F_1 as compared to F_2 levels drops monotonically from a maximum of ≈ 1.6 at low J, down to a value ranging from 1.0 to 1.2. This is in semiquantitative agreement with our prediction (Fig. 7) of a decreasing preference for scattering into the F_1 manifold, and also with the experiments of Zare and co-workers at a lower incident translational energy.[22]

Finally, the experiments of Luntz *et al.*[21] suggest, although the scatter is large, that as the final state rotational angular momentum increases, there will be an increasing tendency to populate preferentially the Λ-doublet levels which are *symmetric* $\Pi(A')$ with respect to reflection of the electronic coordinates in the plane of rotation of the molecule. This is in direct contrast with the present calculations, which indicate a strong propensity for population of the *antisymmetric* $\Pi(A')$ Λ-doublet levels.

IX. DISCUSSION

We have presented here the results of full close-coupling calculations of inelastic transition probabilities for the scattering of NO by a close-packed Ag(111) surface. The interaction was described by the semiempirical potential energy surfaces (PES) determined recently by DePristo and Alexander (DA).[26] The results of these calculations show the same qualitative features (multiple rainbows, preference for scattering into particular fine-structure and Λ-doublet levels) seen in prior theoretical studies.[11,13,18] However, since the present PES are so different from the phenomenological surfaces used previously,[9,11] the quantitative aspects of the final state distributions are significantly different. In particular, we observe a strong tendency for population of the Λ-doublet levels of A'' symmetry with respect to reflection of the electronic coordinates in the plane of rotation of the scattered NO molecule, which is *opposite* to the tendency (seen, albeit less pronounced) in the prior calculations[11,13,18] as well as in the one experimental study of this feature.[21] Also, we observe an equally strong tendency toward preferential population of the lower spin–orbit manifold for low to moderate final J states, which diminishes as J increases to the point where the molecular states are better described in Hund's case (b). This feature is consistent with the predictions of the energy sudden approximation,[7] with the results of the prior scattering calculations,[11,13,18] and with experiment.[21]

The dual potential surface nature of the NO–Ag interaction is a consequence of the electronic degeneracy of the molecule. The results of the present study further reinforce our earlier conclusion[11] that any treatment of the dynamics of the collision of NO with a metal surface which ignores this aspect of the problem will be only approximate and likely will give little information on the true nature of the interaction potentials. We believe this to be true, even if the results of these approximate treatments agree well with suitably averaged experimental quantities. This conclusion will be especially relevant if the dependence of the interaction potential on the orientation of the singly filled π^* orbital of NO is substantial, as predicted by the corrected effective medium calculations of DA.[26]

The dependence of the present PES on the in-plane position of the molecule above the surface, allowed us to simulate in a simplistic way, without taking into account any quantum interference effects, the effect of surface corrugation on these features. We found that the oscillations in the fine-structure averaged final state distributions due to the multiple rotational rainbows were strongly effected. This implies, of course, that the approximation of a flat surface in the simulation of these final state distributions is not justifiable. By contrast, the spin–orbit and Λ-doublet propensities were little effected by the averaging over surface sites. This suggests that these features are reflective of a more fundamental aspect of the NO–Ag interaction which is invariant with respect to the lateral position of the molecule above the Ag(111) unit cell.

Although the CEM PES surfaces used explicitly depend on the position of the NO molecule above the unit cell, there is no explicit dependence on the position of the metal atoms. This is because the calculations were carried out for silver clusters of fixed geometry.[26] To study the physically important effect of energy exchange with a surface in motion would require many additional CEM calculations for a series of varying cluster geometries.

Since the strongest manifestation of the spin–orbit and Λ-doublet propensities were seen for transitions between initial and final molecular rotational levels which are not directly coupled by the interaction potential, it is impossible to explain these propensities by arguments based on inspection of the coupling matrix elements, which have been successful for gas-phase collisions.[48] Rice and co-workers[13] and Lemoine and Corey[17,18] have shown how time-dependent methods can be used to gain mechanistic information on the flow of flux among the NO rotational states as the molecule approaches and recedes from the surface. Hopefully, additional application of similar techniques can provide insight into the origin of the observed fine-structure propensities. Also, we encourage further, precise experimental investigation of the fine-structure dependence of the scattered beam intensity.

As discussed in the preceding section, the results of the present calculations do not yield entirely satisfactory agreement with the most highly resolved experimental results,[21] particularly in the final-state Λ-doublet propensities. This disagreement could reflect (a) inadequacies in the CEM PES used here, (b) the interplay between surface atom motion and the collision of the NO molecule, or (c) the importance of hole-pair, or other not purely electrostatic, interactions. As we have stated previously, rather than attempt to modify the potential to obtain better agreement with experiment, we prefer to offer the present results unaltered. They show clearly the importance and implications of a correct consideration of the role of the dual NO–Ag(111) PES and stand as benchmarks for the calibration of the accuracy of more approximate methods. Only if these can reproduce ac-

curately the present fully-quantum transition probabilities for scattering of NO off a flat surface, can one then trust the extension of these methods to the more difficult treatment of the coupling between surface motion and the collision of the NO molecule.

Additional scattering calculations based on the PES of DA are planned, to investigate the dependence of the NO final state distributions on energy, and, ultimately, on the vibrational motion of the NO molecule. In similar work these PES could be used to model desorption of NO from Ag(111), to provide insight into the nonstatistical fine-structure populations seen in desorption from other substrates.[24,25]

ACKNOWLEDGMENTS

The author would like to thank the U.S. Army Research Office for partial support of this work under Contract No. DAAL03-88-K-0031, and the Alexander von Humboldt foundation for a Senior U.S. Scientist Award, during the tenure of which some of the initial research reported here was accomplished at the Fakultät für Chemie, Universität Bielefeld, Federal Republic of Germany. The scattering calculations were carried out on the VAX11/785 + FPS-M64 system at the Center for Intensive Computation at the University of Maryland. The author is grateful to Professors Andrew DePristo and Gregory Corey for their encouragement and for helpful comments.

[1]H. Voges and R. Schinke, Chem. Phys. Lett. **95**, 221 (1983).
[2]H. Voges and R. Schinke, Chem. Phys. Lett. **100**, 245 (1983).
[3]J. A. Barker, A. W. Kleyn, and D. J. Auerbach, Chem. Phys. Lett. **97**, 9 (1983).
[4]S. Tanaka and S. Sugano, Surf. Sci. **136**, 488 (1984), 143, L371.
[5]E. Zamir and R. D. Levine, Chem. Phys. Lett. **104**, 143 (1984).
[6]J. G. Lauderdale, J. F. McNutt, and C. W. McCurdy, Chem. Phys. Lett. **107**, 43 (1984).
[7]M. H. Alexander, J. Chem. Phys. **80**, 3485 (1984).
[8]G. C. Corey and W.-K. Liu, Surf. Sci. **148**, 675 (1984).
[9]C. W. Muhlhausen, L. R. Williams, and J. C. Tully, J. Chem. Phys. **83**, 2594 (1985).
[10]R. Schinke and R. B. Gerber, J. Chem. Phys. **82**, 1567 (1985).
[11]J. E. Smedley, G. C. Corey, and M. H. Alexander, J. Chem. Phys. **87**, 3218 (1987).
[12]G. C. Corey, J. E. Smedley, M. H. Alexander, and W.-K. Liu, Surf. Sci. **191**, 203 (1987).
[13]B. M. Rice, B. C. Garrett, P. K. Swaminathan, and M. H. Alexander, J. Chem. Phys. **90**, 575 (1989).
[14]S. Holloway and D. Halstead, Chem. Phys. Lett. **154**, 181 (1989).
[15]M. G. Tenner, E. W. Kuipers, A. W. Kleyn, and S. Stolte, Surf. Sci. **211/212**, 819 (1989).
[16]G. C. Corey and D. Lemoine, Chem. Phys. Lett. **160**, 324 (1989).
[17]D. Lemoine and G. C. Corey, J. Chem. Phys. **94**, 767 (1991).
[18]D. Lemoine and G. C. Corey, J. Chem. Phys. **92**, 6175 (1990).
[19]M. G. Tenner, Ph.D. thesis, FOM-Institute for Atomic and Molecular Physics, The Netherlands (1990).
[20]G. Herzberg, *Spectra of Diatomic Molecules*, 2nd ed. (Van Nostrand, Princeton, 1968).
[21]A. C. Luntz, A. W. Kleyn, and D. J. Auerbach, J. Chem. Phys. **76**, 737 (1982).
[22]G. D. Kubiak, J. E. Hurst, Jr., H. G. Rennagel, G. M. McClelland, and R. N. Zare, J. Chem. Phys. **79**, 5163 (1983).
[23]S. R. Cohen, R. Naaman, and G. G. Balint-Kurti, Chem. Phys. Lett. **134**, 119 (1989).
[24]L. J. Richter, S. A. Buntin, R. R. Cavanagh, and D. S. King, J. Chem. Phys. **89**, 5344 (1988).
[25]F. Budde, A. V. Hamsa, P. M. Ferm, G. Ertl, D. Weide, P. Andresen, and H.-J. Freund, Phys. Rev. Lett. **60**, 1518 (1988).
[26]A. E. DePristo and M. H. Alexander, J. Chem. Phys. **94**, 8454 (1991).
[27]T. J. Raeker and A. E. DePristo, Int. Rev. Phys. Chem. (1990).
[28]J. D. Kress and A. E. DePristo, J. Chem. Phys. **88**, 2596 (1988).
[29]J. D. Kress, M. S. Stave, and A. E. DePristo, J. Phys. Chem. **93**, 1556 (1989).
[30]T. J. Raeker and A. E. DePristo, Phys. Rev. B **39**, 9967 (1989).
[31]T. J. Raeker and A. E. DePristo, Surf. Sci. **235**, 84 (1990).
[32]D. M. Brink and G. R. Satchler, *Angular Momentum*, 2nd ed. (Clarendon, Oxford, 1968).
[33]A FORTRAN program to compute the Legendre expansion coefficients in Eqs. (11) and (12) is available on request from the author by electronic mail (address: mha@hibridon.umd.edu). Please supply a return electronic mail address.
[34]R. N. Zare, A. L. Schmeltekopf, W. J. Harrop, and D. L. Albritton, J. Mol. Spectrosc. **46**, 37 (1973).
[35]M. H. Alexander and P. J. Dagdigian, J. Chem. Phys. **80**, 4325 (1984).
[36]J. M. Brown, J. T. Hougen, K.-P. Huber, J. W. C. Johns, I. Kopp, H. Lefebvre-Brion, A. J. Merer, D. A. Ramsay, J. Rostas, and R. N. Zare, J. Mol. Spectrosc. **55**, 500 (1975).
[37]H. Lefebvre-Brion and R. W. Field, *Perturbations in the Spectra of Diatomic Molecules* (Academic, New York, 1986).
[38]J. T. Hougen, Natl. Bur. Stand. (U.S.) Monogr. 115 (1970).
[39]K. P. Huber and G. Herzberg, *Molecular Spectra and Molecular Structure. IV. Constants of Diatomic Molecules* (Van Nostrand Reinhold, New York, 1979).
[40]D. E. Fitz, L. H. Beard, and D. J. Kouri, J. Chem. Phys. **59**, 257 (1981).
[41]G. Wolken, J. Chem. Phys. **59**, 1159 (1973); **62**, 2730 (1975).
[42]D. J. Kouri and R. B. Gerber, Isr. J. Chem. **22**, 321 (1982).
[43]HIBRIDON is a package of programs for the time-independent quantum treatment of inelastic collisions and photodissociation written by M. H. Alexander, D. Manolopoulos, H.-J. Werner, and B. Follmeg, with contributions by P. F. Vohralik, D. Lemoine, G. Corey, B. Johnson, T. Orlikowski, and W. Kearney.
[44]J. J. Dongarra, *Performance of Various Computers Using Standard Linear Equations Software*, Computer Science Department, University of Tennessee, Knoxville, TN 37996-1301, November 1990.
[45]R. Schinke, J. Chem. Phys. **76**, 2352 (1982).
[46]M. H. Alexander, P. Andresen, R. Bacis, R. Bersohn, F. J. Comes, P. J. Dagdigian, R. N. Dixon, R. W. Field, G. W. Flynn, K.-H. Gericke, B. J. Howard, J. R. Huber, D. S . King, J. L. Kinsey, K. Kleinermanns, A. C. Luntz, A. J. MacCaffery, B. Pouilly, H. Reisler, S. Rosenwaks, E. Rothe, M. Shapiro, J. P. Simons, R. Vasudev, J. R. Wiesenfeld, C. Wittig, and R. N. Zare, J. Chem. Phys. **89**, 1749 (1988).
[47]R. G. Macdonald and K. Liu, J. Chem. Phys. **91**, 821 (1989).
[48]P. J. Dagdigian, M. H. Alexander, and K. Liu, J. Chem. Phys. **91**, 839 (1989).
[49]T. R. Proctor, D. J. Kouri, and R. B. Gerber, J. Chem. Phys. **80**, 3845 (1984).
[50]R. C. Mowrey, H. F. Bowen, and D. J. Kouri, J. Chem. Phys. **86**, 2441 (1987).
[51]R. C. Mowrey and D. J. Kouri, J. Chem. Phys. **84**, 6466 (1986).
[52]A. W. Kleyn, A. C. Luntz, and D. J. Auerbach, Surf. Sci. **117**, 33 (1982).